

Estimation of the Surface Area Covered by Snow and The Resulting Runoff using Landsat Satellite Images [†]

Kiana Kazari, Reza Shah-Hosseini * and Sara khanbani

School of Surveying and Geospatial Engineering, College of Engineering, University of Tehran, Tehran, Iran

* Correspondence Email: rshahosseini@ut.ac.ir.

Abstract: Snow is one of the most important sources of water in most parts of the world, which supplies about a third of the water needed for agricultural activities, drinking, and underground water sources. The runoff caused by melted snow can be destructive, also the numerous volume of snow can lead to an avalanche, so it's important to estimate it. The area of the snow research is around Goose Lake in California, the USA where the ground snow measuring station is (Latitude: 41.92999, Longitude: -120.4168117). The snow can be measured and calculated using the Daily Satellite imagery of the Landsat for five years' period (2017–2022) for about four months (December–March) (total of about 40 images). The information from ground snow measuring stations was used to evaluate the final results. The accuracy assessment shows 76% accuracy.

Keywords: remote sensing; snow depth; landsat images; NDSI Index; snow cover fraction

1. Introduction

Snow is a mixture of ice crystals and water. Snow covers up to 53% of the Earth's surface in the Northern Hemisphere and up to 44% of the Earth's surface in the Southern Hemisphere throughout the year. (The country of America, which is the region studied in this article, is located in the northern hemisphere). At least one-third of the water used to irrigate agricultural lands in the world comes from runoff caused by the melting of fallen snow. Today, the effects of snow and the resulting runoff have become more important due to the impact on agriculture and its products and causing floods and avalanches. When it snows, it can freeze agricultural crops and the fertile soil of the region, during which the soil loses its fertility and destroys the agricultural crops. For these reasons, if the amount of snowfall in a region is estimated and according to algorithms and patterns, the area and the amount of snowfall in the desired area is estimated, they can help farmers in days and even in the same time frame. Next year, necessary and preventive measures should be taken to prevent the destruction of agricultural products and soil.

Other effects of snow and runoff include floods and avalanches. When it snows, surveyors can estimate the probability of an avalanche by using sensor images taken from that area at certain hours and days and calculating the area and volume of snow. Also, by calculating the amount of runoff produced from snow, they can predict the probability and volume of floods. Snow depth can provides quantitative information about snow material and energy. Snow depth measurement methods based on station observations are highly accurate, but these methods cannot give the spatiotemporal changes of snow depth in the observation stations, because the observation stations are often sparse. The ability to access vast databases using remote sensing data has provided a fast and effective way to continuously monitor snow depth in all weather conditions and with high time resolution.

In the field of remote sensing, it is assumed that electromagnetic radiation from snow has a direct relationship with the depth of snow. Different methods have been provided

Citation: Lastname, F.; Lastname, F.; Lastname, F. Title. *Proceedings* **2022**, *69*, x. <https://doi.org/10.3390/xxxxx>

Academic Editor: Firstname Lastname

Published: date

Publisher's Note: MDPI stays neutral with regard to jurisdictional claims in published maps and institutional affiliations.



Copyright: © 2022 by the authors. Submitted for possible open access publication under the terms and conditions of the Creative Commons Attribution (CC BY) license (<https://creativecommons.org/licenses/by/4.0/>).

to estimate the depth of snow. Tang et al. have developed an algorithm depends on a linear relationship between snow depth and temperature brightness. This algorithm was improved by various researchers, for example, Foster considered foster and terrain parameters to improve snow depth. In the article presented by Gan et al., it was suggested that the relationship between snow depth and temperature brightness is non-linear, and in the same way, using non-linear methods such as using artificial neural networks, non-linear relationships between lighting parameters and other optional parameters were created. Daeseong et al. used Landsat and MODIS images to estimate snow depth. In their proposed method, several functions were analyzed to investigate the relationship between snow depth and Snow Cover Fraction.

Due to the mentioned reasons, for the continuous and accurate monitoring of the amount of snowfall and the calculation of the resulting runoff, there is a need for satellite images with a not-very long sensor return period and also with high resolution. Also, the purpose of using satellite images is to receive and extract information regarding snow parameters, a sensor whose images include thermal bands should be used so that snow-covered areas can be distinguished and extracted from other areas. One of the famous sensors suitable for processing snow-covered images is the Landsat 8 sensor, and its return period is 16 days.

Using the NDSI index and the NDVI index, the normalized index of the difference and changes in snow cover and vegetation, on Landsat sensor images, the snow surface is determined in the photo without cloud cover. The desired image prepared in this project is a satellite image that was taken from the United States of America, the city of California, and near Goose Lake in 4 months (December–March) from 2017 to 2022, and it has snow cover. The image used in this article is from the second series of Landsat sensor products (which are in the form of 16-day periods).

2. Data & Study Area

2.1. Study Area

Goose Lake region in latitude 41.92999 and longitude -120.4168117 has been selected as the study area. The time selected for this study is 2017 to 2022. This region is located at latitude 41.92999, as a result, it is a region that is considered one of the cold regions and due to weather conditions, snow cover is seen in this region.

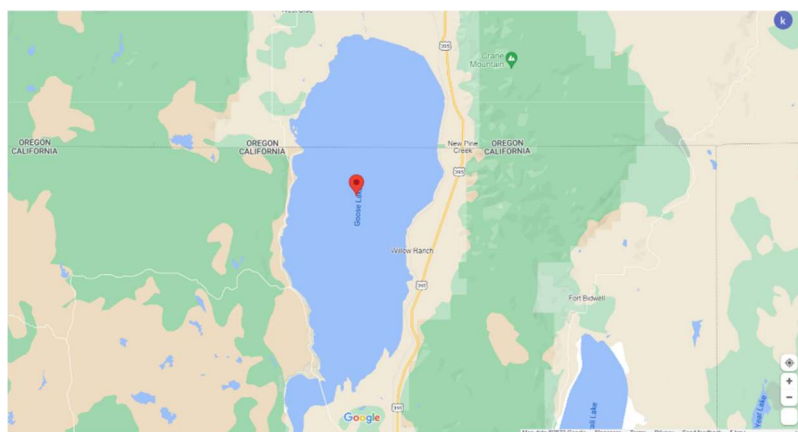


Figure 1. Goose Lake map

2.2. Data

This study used remotely sensed and in-situ data sets. Remotely sensed data comprises Landsat8-TM (spatial resolution 30 meters), acquired from 2017 to 2022 obtained

through the google earth engine platform. Table 1 showed additional information on the remotely sensed dataset.

Table 1. Satellite data description.

Satellite	Acquired time from-to
Landsat8/TM	From 12/2017 to 03/2022

In-situ snow depth observations were acquired from the USDA (U.S. Department of Agriculture). There are four stations in the mentioned study area. Table 2 described the information of in-situ data.

Table 2. In-situ dataset description.

Station name	Lat/long	Time
Crowder Flat	41.89/-120.75	From 12/2017 to 03/2022
Dismal Swamp	41.99/-120.18	From 12/2017 to 03/2022
State Line	41.99/-120.72	From 12/2017 to 03/2022
Strawberry	42.13/-120.84	From 12/2017 to 03/2022

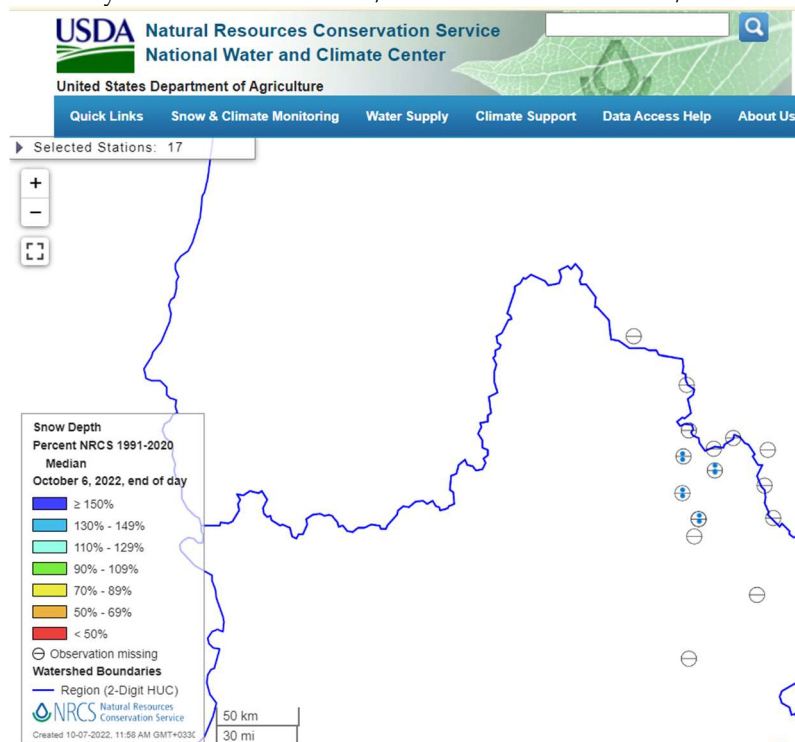


Figure 2. Ground Station Distribution map from USDA website.

3. Methodology

The conceptual model of the proposed method is presented according to the flowchart of the Figure 3.



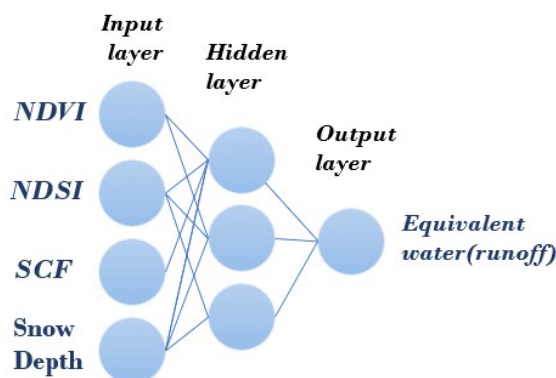


Figure 3. Detailed work flowchart in developing the snow depth map from Landsat images.

In this method, first, Landsat images related to December, January, February, and March of 2017 to 2022, which had less than 10% cloud cover, were downloaded. Then their NDSI images have been calculated according to the following equation:

$$NDSI = \frac{\text{Green band} - \text{SWIR band}}{\text{Green band} + \text{SWIR band}} \quad (1)$$

In this equation, green band and SWIR band respectively correspond to bands 3 and 6 of Landsat 8 image. NDSI measures the relative value of the reflectance difference between the Green and SWIR bands and controls the variance between the 2 bands, which is useful for the field of snow mapping. Snow is not reflective only in the visible range, and it also has high absorption in NIR or SWIR. This parameter helps a lot to separate between clouds and snow. Another parameter used in this study to estimate snow depth is NDVI. NDVI is an index sensitive to vegetation and due to the existence of vegetation in the region, it can be important for separating snowy areas.

The NDVI index is calculated according to the following equation:

$$NDVI = \frac{\text{NIR band} - \text{R band}}{\text{NIR band} + \text{R band}} \quad (2)$$

In this equation, the NIR band and R band respectively correspond to bands 4 and 5 of Landsat 8 image. According to the calculated NDSI and NDVI images of two regions for different times, SCF was produced by the formula presented in the article “Mapping Snow Depth Using Moderate Resolution Imaging Spectroradiometer Satellite Images: Application to the Republic of Korea”, which combines NDVI and NDSI to build snow cover map.

$$SCF = \begin{cases} 0.58e^{-23.1(NDSI - 0.68)^2} + 0.42e^{-286.68(NDVI - 0.06)^2} & NDSI \leq 0.68, NDVI \geq 0.06 \\ 0.58e^{-23.1(NDSI - 0.68)^2} + 0.42 & NDSI \leq 0.68, NDVI < 0.06 \\ 0.58 + 0.28e^{-286.68(NDVI - 0.06)^2} & NDSI > 0.68, NDVI \geq 0.06 \\ 1 & NDSI > 0.68, NDVI < 0.06 \end{cases} \quad (3)$$

After calculating SCF, the relationship between snow depth and SCF is estimated. According to the studies, the relationship between snow depth and SCF is an exponential

relationship or linear form, so it is necessary to investigate an exponential function and linear function for this purpose. According to the formulas: (4–6).

$$\text{Snow Depth} = a * (\text{SCF}) + b \tag{4}$$

$$\text{Snow Depth} = a * \exp(b * \text{SCF}) \tag{5}$$

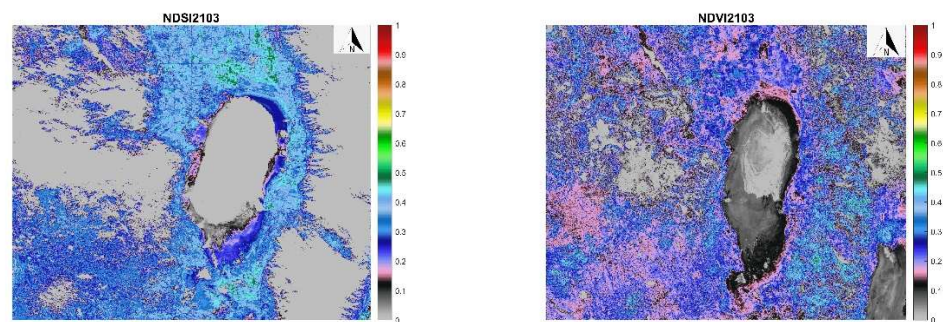
$$\text{Snow Depth} = a * \exp(b * \text{SCF}) + c * \exp(d * \text{SCF}) \tag{6}$$

To calculate a, b, c, d unknown parameter of equation (4–6), equivalent values of ground stations are used. The 30 pieces of information related to three stations were used to calculate the coefficients α and β and the information about the station and 50 other pieces of information about stations were used to evaluate the accuracy. For accuracy evaluation, the RMSE parameter is used, which provides the difference between the values at the station and the calculated values.

In the next step calculated Snow depth, SCF, NDSI and NDVI applied to estimate equivalent snow water in the study area. Multi-layer perceptron applied to create relationship between aforementioned parameters. Figure 3 shows schematic presentation of proposed method. A multilayer perceptron is a fully connected class of feedforward artificial neural networks. If a multilayer perceptron has a linear activation function in all neurons, that is, a linear function that maps the weighted inputs to the output of each neuron, then linear algebra shows that any number of layers can be reduced to a two-layer input-output model. Learning occurs in the perceptron by changing connection weights after each piece of data is processed, based on the amount of error in the output compared to the expected result.

4. Results

According to the proposed method, the outputs of NDVI, NDSI, SCF and Snow depth related to the march of 2021 are given in Figure 4.



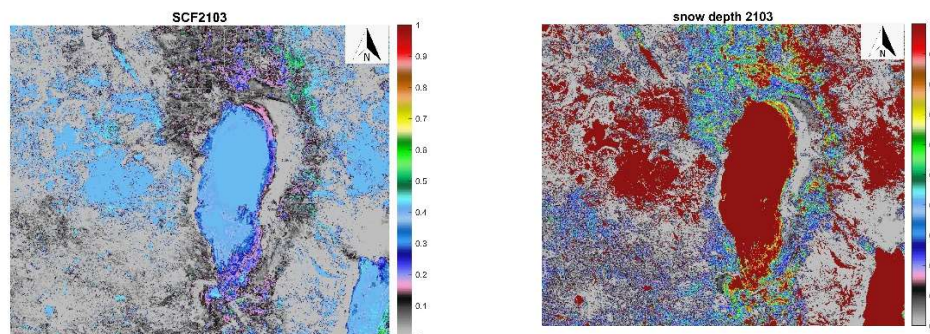


Figure 4. NDSI, NDVI, SCF, Snow Depth images from March 2021.

Table 3 shows some of the training data in order to clarify the estimation problem. In this Table Snow depth in _Situ provided from USDA website and considered as a reference criterion to calculate accurate equation models, related to calculated Snow Cover Fraction (Equations (4–6)).

Table 3. the example of some training data to compute relationship between Snow Depth and SCF.

Station Id	Station Name	NDVI	NDSI	Latitude	Longitude	Snow Depth(in-Situ)	SCF(calculated)
977	Crowder Flat	0.5274	-0.587	41.89	-120.75	2.75×10^{-5}	5.91×10^{-6}
977	Crowder Flat	0.06	-0.477	41.89	-120.75	2.258635	0.42
977	Crowder Flat	0	-0.13	41.89	-120.75	2.258635	0.42
446	Dismal swamp	0.26	-0.771	41.99	-120.18	2.05×10^{-5}	4.40×10^{-6}
446	Dismal swamp	0.195	-0.327	41.99	-120.18	0.010533	0.00226
446	Dismal swamp	0.258	-0.015	41.99	-120.18	6.42×10^{-5}	1.38×10^{-5}

Based on the investigation, the linear and exponential relationship between in-situ snow depth and calculated snow cover fraction (figure) calculated Using 30 corresponding data the value of a, b, c and d is estimated using the least square method. Equation (7–9) indicate the estimated formulas for linear, first order exponential function and second order exponential function respectively.

$$\text{Snow depth} = a * (\text{SCF}) + b \tag{7}$$

$$a = 5.426$$

$$b = -0.0113$$

$$\text{Snow Depth} = a * \exp(b * \text{SCF}) \tag{8}$$

Coefficients (with 95% confidence bounds):

$$a = 0.3699 (0.2377, 0.5021)$$

$$b = 4.159 (3.364, 4.953)$$

$$\text{Snow Depth} = a \cdot \exp(b \cdot \text{SCF}) + c \cdot \exp(d \cdot \text{SCF}) \tag{9}$$

Coefficients (with 95% confidence bounds):

$$a = -6.95 (-6.95, -6.95)$$

$$b = -4.326e-06 (-1.9e-05, 1.035e-05)$$

$$c = 6.95 (6.95, 6.95)$$

$$d = 0.67 (0.67, 0.67)$$

In order to evaluate the estimated parameters of 50 in-situ snow depth data with them Corresponded snow cover fraction used to calculate root mean square error (RMSE). According to the result the RMSE for linear function is equal to 0.0166 meters which is an acceptable value. The RMSE for first order exponential function (equation 8) is equal 0.2502 meters. And the RMSE for second order exponential function is equal to 1.86e-08 meters.

According to the result the second order exponential function provide better result compare to linear and first order exponential function. The Figure 5 shows the fitness of second order exponential function on the inputs data. The figure also shows optimized curve for exponential fits based on the current data set.

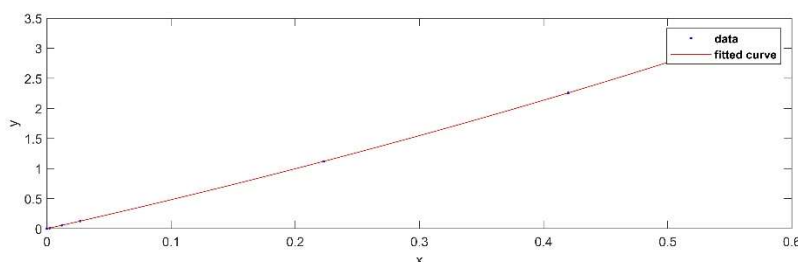


Figure 5. the second order exponential curve fitted on the current data set.

After calculating snow depth, artificial neural network with 3 layers (input-hidden and output layer) defined to estimate equivalent water (snow depth water). The input layer includes 4 neurons (NDVI, SCF, NDSI, Snow Depth), the hidden layer includes 3 neurons and output layer include 1 neuron corresponded to equivalent snow water. Sigmoid function set as activation function and different learning rate, epoch number and hidden layer’s neurons tested to sensitivity analysis of proposed network. According to the results the RMSE equal to 0.32069, 0.309, 0.3918, 0.27, 0.273, 0.543, 0.257, 0.251 meter for 0.3, 0.6, 0.1, 0.7, 0.8, 0.01, 0.9, 0.95 learning rates respectively. According to the result the learning rate set equals to 0.95 shows better result. In the next step the epoch numbers tested to select optimum epoch numbers. The RMSE equals to 0.246, 0.246, 0.245, 0.247 meter for 4, 6, 10, 20 epoch numbers respectively. The result show stable result against different epoch numbers. When the neurons of hidden layer set 1 the RMSE is equal to 0.247 meter, if the neurons equal to 2 the RMSE is 0.243 and if the neurons equal to 3 the RMSE is 0.242 meter. The results is stable for the number of neurons in hidden layer and the number of epochs.

5. Conclusion

The paper proposed the snow depth parameter calculation based on the snow cover fraction parameter. Snow cover fraction calculated using NDVI and NDSI index. According to the result the second order exponential function shows the best fitness between calculated Snow Depth and ground station Snow depth. The equivalent water (run off) can be estimated based on NDVI, NDSI, SCF and snow depth parameters. The artificial neural network considered as a powerful method in order to investigate the relationship between these parameters.

Reference

1. Daeseong Kim*, and Hyung - Sup Jung (2018). "Mapping Snow Depth Using Moderate Resolution Imaging Spectroradiometer Satellite Images: Application to the Republic of Korea." Department of Geoinformatics, University of Seoul.
2. R. Tong *, J. Parajka, J. Komma, G. Blöschl (2020). "Mapping snow cover from daily Collection 6 MODIS products over Austria." Institute of Hydraulic Engineering and Water Resources Management, Vienna University of Technology, Karlsplatz 13/222, 1040 Vienna, Austria.
3. Jing Guo, Ziti Jiao, Lei Cui, Siyang Yin, Yaxuan Chang, Rui Xie, Sijie Li, Zidong Zhu (2020), "A METHOD TO IDENTIFY HIGH-QUALITY PURE SNOW DATA IN POLDER DATABASE," State Key Laboratory of Remote Sensing Science, College of Remote Sensing and Engineering, Faculty of Geographical Science, Beijing Normal University, Beijing 100875, China.
4. Daeseong Kim*, Hyung - Sup Jung*† and Jeong-Cheol Kim** (2017), "Comparison of Snow Cover Fraction Functions to Estimate Snow Depth of South Korea from MODIS Imagery," *Department of Geoinformatics, University of Seoul **National Institute of Ecology, Riparian Ecosystem Research Team.
5. Romanov, P. and D. Tarpley, 2007. Enhanced algorithm for estimating snow depth from geostationary satellites, Remote sensing of environment, 108(1): 97-110.
6. Salomonson, V.V. and I. Appel, 2006. Development of the Aqua MODIS NDSI fractional snow cover algorithm and validation results, IEEE Transactions on geoscience and remote sensing, 44(7): 1747-1756.
7. Lin, J., X. Feng, P. Xiao, H. Li, J. Wang, and Y. Li, 2012. Comparison of snow indexes in estimating snow cover fraction in a mountainous area in northwestern China, IEEE Geoscience and Remote Sensing Letters, 9(4): 725-729.
8. Roy, A.; Royer, A.; Turcotte, R. Improvement of springtime stream-flow simulations in a boreal environment by incorporating snow-covered area derived from remote sensing data. J. Hydrol. 2010, 390, 35–44.
9. Ault, T.W., Czajkowski, K.P., Benko, T., Coss, J., Struble, J., Spongberg, A., Templin, M., Gross, C., 2006. Validation of the MODIS snow product and cloud mask using student and NWS cooperative station observations in the Lower Great Lakes Region. Remote Sens. Environ. 105, 341–353.
10. Da Ronco, P., Avanzi, F., De Michele, C., Notarnicola, C., Schaeffli, B., 2020. Comparing MODIS snow products Collection 5 with Collection 6 over Italian Central Apennines. Int. J. Remote Sens. 41 (11), 4174–4205.
11. Dong, C., 2018. Remote sensing, hydrological modeling and in situ observations in snow cover research: A review. J. Hydrol. 561, 573–583.
12. Gao, Y., Xie, H., Yao, T., Xue, C., 2010. Integrated assessment on multi-temporal and multi-sensor combinations for reducing cloud obscuration of MODIS snow cover products of the Pacific Northwest USA. Remote Sens. Environ. 114, 1662–1675.
13. Grayson, R., Blöschl, G., 2001. Spatial patterns in catchment hydrology: observations and modelling. CUP Archive.
14. Hall, D.K., Riggs, G.A., 2011. Normalized-Difference Snow Index (NDSI). In: Singh, V.P., Singh, P., Haritashya, U.K. (Eds.), Encyclopedia of Snow, Ice and Glaciers. Springer, Netherlands, Dordrecht, pp. 779–780. <https://doi.org/10.1007/978-90-481-2642-2>.
15. Hall, D.K., Riggs, G.A., DiGirolamo, N.E., Román, M.O., 2019. Evaluation of MODIS and VIIRS cloud-gap-filled snow-cover products for production of an Earth science data record. Hydrol. Earth Syst. Sci. 23 (12), 5227–5241. <https://doi.org/10.5194/hess23-5227-2019>.
16. Tedesco, M., J. Pulliainen, M. Takala, M. Hallikainen, and P. Pampaloni, 2004. Artificial neural network-based techniques for the retrieval of SWE and snow depth from SSM/I data, Remote Sensing of Environments, 90(1): 76-85.